

# Repulsive trap for two electrons in a magnetic field

A. D. Chepelianskii<sup>1</sup> and D. L. Shepelyansky<sup>2</sup><sup>1</sup>*Lycée Pierre de Fermat, Parvis des Jacobins, 31068 Toulouse Cedex 7, France*<sup>2</sup>*Laboratoire de Physique Quantique, UMR 5626 du CNRS, Université Paul Sabatier, 31062 Toulouse Cedex 4, France*

(Received 1 November 2000; published 3 April 2001)

We study numerically and analytically the dynamics of two classical electrons with Coulomb interaction in a two-dimensional antidot superlattice potential in the presence of crossed electric and magnetic fields. It is found that near one antidot the electron pair can be trapped for a long time, and the escape rate from such a trap is proportional to the square of a weak electric field. This is qualitatively different from the case of noninteracting electrons which are trapped forever by the antidot. For pair propagation in the antidot superlattice, we found a broad parameter regime for which the pair is stable, and where two repulsive electrons propagate together for an enormously large distance.

DOI: 10.1103/PhysRevB.63.165310

PACS number(s): 72.20.My, 45.05.+x, 05.45.Mt

## I. INTRODUCTION

Recent technological developments allowed one to create various types of surface superlattices for two-dimensional (2D) electron gas in semiconductor heterostructures, and to investigate their transport properties in the presence of a magnetic field. Experiments with antidot lattices were carried out by different experimental groups (see, e.g., Refs. 1–4), and the contribution of classical periodic orbits in the resistivity peaks at certain values of magnetic field was clearly identified. In fact, the size of the antidots and the distance between them are relatively large, and an analysis of classical trajectory dynamics can be successfully applied to understand a number of unusual transport properties in such antidot arrays.<sup>5,6</sup> Due to the nonlinearity of motion in the vicinity of an antidot potential, the classical dynamics can be chaotic, which leads to diffusive spreading of trajectories even for perfectly periodic lattices.<sup>5,6</sup> If the distance between antidots is large or comparable to the cyclotron radius of an electron in a magnetic field perpendicular to the lattice, then one should first understand, the properties of electron dynamics near one antidot. In the absence of an electric field, the dynamics is integrable for an antidot of circular shape due to angular momentum conservation, and an electron always regularly rotates around the antidot. An electric field applied in the 2D plane of the superlattice breaks the cylindrical symmetry, and can lead to electron escape from the antidot to infinity. The problem of electron dynamics, in crossed electric  $E$  and magnetic  $B$  fields near a circular elastic disk (antidot), was studied in Ref. 7. It was shown that the dynamics can be described by a simple area-preserving map which depends only on one dimensionless parameter  $\epsilon = (2\pi m/ae)(E/B^2)$ , where  $m$  and  $e$  are electron mass and charge, and  $a$  is the disk radius. For small  $\epsilon < \epsilon_c$  the electron dynamics in a phase space of angular momentum  $l$  and a conjugated angle  $\phi$  is bounded by the invariant Kolmogorov-Arnold-Moser (KAM) curves so that the electron always remains near the disk. Conversely, for  $\epsilon > \epsilon_c$  the KAM curves are destroyed, global chaos sets in, and the electron escapes to infinity after a few collisions with the disk.

Until now the classical dynamics in antidot lattices was

studied only for noninteracting electrons.<sup>5–7</sup> In this paper, we analyze the effect of Coulomb interaction between classical electrons in the vicinity of an antidot. We show that, for sufficiently strong interaction between electrons, their dynamics becomes chaotic. Due to this, one or two electrons can escape from the antidot, even in an arbitrary weak applied electric field  $E$  that corresponds to  $\epsilon_c \rightarrow 0$  contrary to  $\epsilon_c > 0$  in the absence of interaction. We determine the dependence of the average escape rate  $\Gamma$  on  $\epsilon$ , showing that, in the limit of a small electric field,  $\Gamma \propto \epsilon^2$ . After this we also discuss two-electron propagation in the antidot superlattice.

The paper is organized as follows. In Sec. II we briefly discuss the one-electron dynamics near the antidot in crossed magnetic and electric fields. In Sec. III the dynamics of two interacting electrons is analyzed in detail. The electron motion in the antidot superlattice is considered in Sec. IV. In Sec. V we summarize the obtained results.

## II. ONE-ELECTRON DYNAMICS

The dynamics of an electron in crossed electric and magnetic fields in two dimensions with one antidot is described by the Hamiltonian

$$H_0 = (\mathbf{p} - e\mathbf{A})^2/2m + U(x, y) - e\mathbf{E}\mathbf{r}, \quad (1)$$

where  $\mathbf{A}$  is the vector potential, and  $U(x, y)$  describes an antidot potential which depends only on the radius  $r = \sqrt{x^2 + y^2}$  with  $U = 0$  for  $r \geq a$ . For convenience, following Ref. 5, we introduce the dimensionless variables  $\tilde{x} = x/a$ ,  $\tilde{y} = y/a$ ,  $\tilde{t} = t/\tau_0$ ,  $\tilde{H}_0 = H_0/2\epsilon_F$ ,  $\tilde{U} = U/2\epsilon_F$ ,  $\tilde{B} = B/B_0$ , and  $\tilde{E} = E/E_0$  where  $\epsilon_F(v_F)$  is the Fermi energy (velocity),  $\tau_0 = (2\epsilon_F/ma^2)^{-1/2} = a/v_F$ , and the magnetic and electric fields are scaled by  $B_0 = (m\epsilon_F)^{1/2}/ea$  and  $E_0 = 2\epsilon_F/ea$ , respectively. In these units a magnetic field  $B = B_0$  gives the cyclotron radius  $R_c = a$  for an electron with energy  $\epsilon_F = mv_F^2/2$ . We choose the Landau gauge  $\mathbf{A} = (-By, 0, 0)$ . Then, omitting the tildes, the Hamiltonian equations of motion read

$$dx/dt = v_x, \quad dv_x/dt = Bv_y - dU/dx - E_x, \quad (2)$$

$$dy/dt = v_y, \quad dv_y/dt = -Bv_x - dU/dy - E_y$$

where  $v_x = p_x + yB$  and  $v_y = p_y$ . To model the antidot, we chose the potential:

$$U(x, y) = U_0(1 - r)^6. \quad (3)$$

Usually we choose  $U_0$  to be much larger than the electron energy  $H_0$ , so that this potential becomes very similar to an absolutely rigid disk with an effective radius  $a_{eff}$  about 15% smaller than  $a$ .

Far from the antidot the equations of motion are exactly solvable, and give an electron rotation over a circle of cyclotron radius  $R_c = v/\omega_c$ , with a cyclotron frequency  $\omega_c = B$ . In addition, this circle moves with the drift velocity  $v_d = E/B$  in a direction perpendicular to the electric and magnetic fields. As found by Berglund *et al.*<sup>7</sup>, near the antidot, the dynamics depends strongly on the dimensionless parameter  $\epsilon = v_d 2\pi/\omega_c = 2\pi E/B^2$ . For  $\epsilon \gg 1$  the electron scatters on the antidot, and escapes to infinity after one collision. Conversely, the situation with not very large  $\epsilon$  is much richer.<sup>7</sup> In this case the electron can collide many times with the antidot, and this process is described by a simple area-preserving map<sup>7</sup>

$$\bar{\phi} = \phi + \pi - 2 \sin^{-1} \beta, \quad (4)$$

$$\bar{\beta} = \beta - \epsilon \sin \bar{\phi},$$

where bars denote the values of variables after collision,  $\phi$  is the scattering angle measured in respect to the direction of the drift velocity, and  $\beta$  is the scattering impact parameter divided by the antidot radius. In this way  $\beta$  varies in the interval  $(-1, 1)$ . We note that  $\beta$  can be also considered as the orbital momentum  $l$  of the electron divided by the maximal momentum  $l_{max} = av$ , at which electron still collides with the antidot. The real dynamics is correctly described by the map if  $R_c \gg 1$ , that corresponds to  $v \gg B$ . For  $\epsilon \ll 1$  the variation of  $\beta$  is bounded by the invariant KAM curves, and the electron is trapped near the antidot. The last KAM curve is destroyed for  $\epsilon > \epsilon_c \approx 0.45$ ,<sup>7</sup> so that orbits with initial  $\beta \approx 0$  can escape from the antidot to infinity. Of course, for  $\epsilon > \epsilon_c$  some islands with regular motion inside still remain, but they become very small as soon as  $\epsilon$  becomes significantly larger than  $\epsilon_c$ .

To study the electron dynamics in Eq. (1), the Hamiltonian equations of motion are solved numerically by a Runge-Kutta method of fourth order, so that the electron energy is conserved with a relative precision better than  $10^{-6}$ . The examples of the Poincaré cross sections constructed at  $x=0$  and  $v_x > 0$ , for trajectories trapped near the antidot, are shown in Figs. 1 and 2. In Fig. 1,  $\epsilon \approx 0.16$  is rather small, and almost all the phase space is filled by integrable KAM curves. For Fig. 2, the parameter  $\epsilon \approx 0.42$  is close to  $\epsilon_c$ , and KAM curves become more deformed and the chaotic component becomes visible. This case can be compared with Fig. 3 in Ref. 7, where the cross section for the map [Eqs. (4)] is given for a close value of  $\epsilon$ . Here we

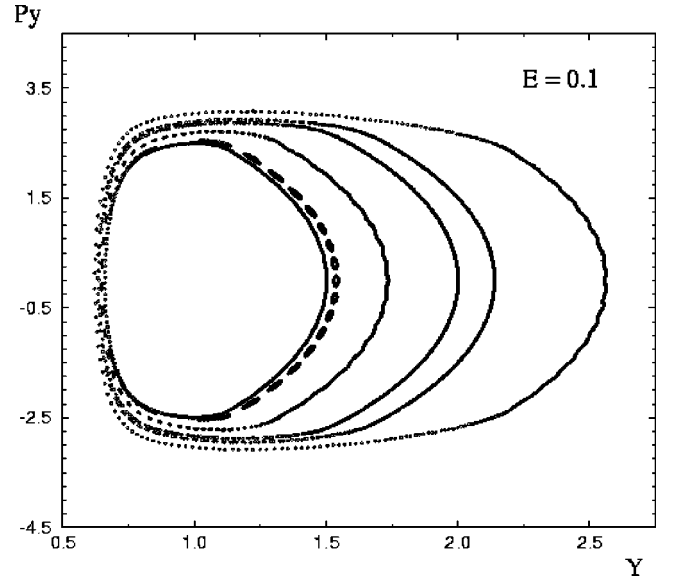


FIG. 1. Poincaré cross section for Hamiltonian (1) constructed at  $x=0$ , and  $v_x > 0$  for  $H_0 = 8.725$ ,  $B = -2$ , and  $E = 0.1$ , so that  $\epsilon \approx 0.16$ . The antidot determined by potential (3) is located at  $(0, 0)$ ;  $U_0 = 1000$ .

should mention that formally the description provided by the map [Eqs. (4)] is valid only at  $v \gg B$ .<sup>7</sup> However, in our numerical simulations we found that the map is already effectively valid for  $v \approx 2B$  (see Figs. 1 and 2). For example, the exact simulations give the escape border  $\epsilon_c$  with 10% accuracy. This result, however, assumes that the potential of the antidot is rather steep. The case with a smooth antidot potential is rather different, as shown in Ref. 5.

It is interesting to note that the map [Eqs. (4)] cannot be valid if orbits have  $|\beta| \approx 1$  or  $|\beta| > 1$ . For example, if the antidot is inside a large cyclotron circle, then the electron will make many rotations before this slowly drifting circle will cross the antidot. This situation is not taken into account by the first equation in Eq. (4). An example of the electron

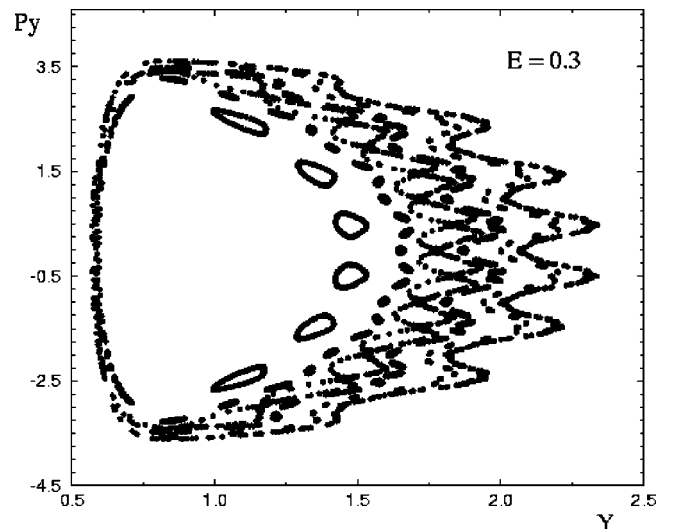


FIG. 2. Same as in Fig. 1, but for  $E = 0.3$  and  $\epsilon \approx 0.42$ .

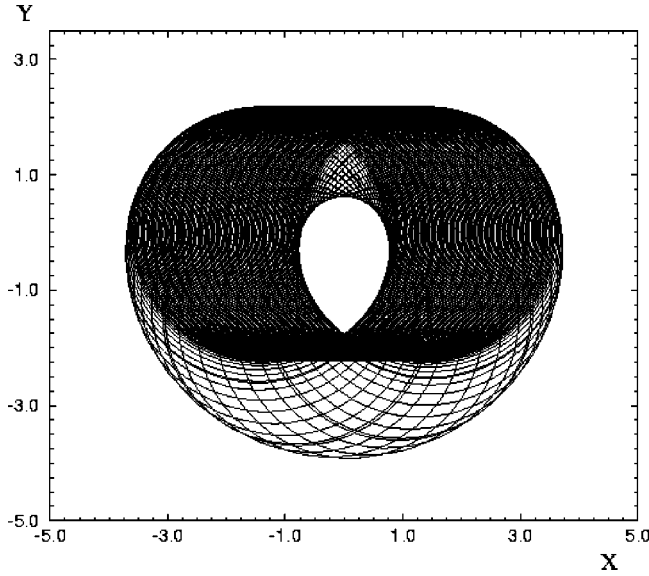


FIG. 3. Electron dynamics in the  $(x, y)$  plane near the antidot of Fig. 1 for  $H_0=9.7$ ,  $B=-2.0$ ,  $E=0.1$ , and  $\epsilon \approx 0.16$ .

dynamics in this case is given in Fig. 3. Here  $\epsilon \approx 0.16$  is small, and the motion is still regular. We should stress that such a trajectory separates orbits which escape to infinity and those which collide with the antidot on each cyclotron period. For an antidot superlattice with an antidot spacing comparable to  $R_c$ , this type of orbit (see Fig. 3) is of special importance, since these orbits can easily jump from one antidot to another, leading to a global diffusion in the system. We will discuss this situation in Sec. III.

### III. EFFECTS OF COULOMB INTERACTION ON ELECTRON DYNAMICS

Let us now consider how the Coulomb interaction between two electrons affects their dynamics near the antidot. In this case the Hamiltonian of the system reads

$$H = H_0(\mathbf{p}_1, \mathbf{r}_1) + H_0(\mathbf{p}_2, \mathbf{r}_2) + e^2/|\mathbf{r}_1 - \mathbf{r}_2|. \quad (5)$$

While in free space the Coulomb interaction repels the electrons and leads to their separation, the situation is more complicated in the presence of a magnetic field. In the case without any antidot the total momentum of the two electrons is conserved, and as a result each electron rotates regularly on a cyclotron circle, which in addition rotates around the center of mass of the system. Without an external electric field ( $E=0$ ) the center of mass is fixed and inert, whereas in the presence of the field ( $|E|>0$ ) the center of mass drifts with a constant velocity  $v_d=E/B$ , but the average distance between electrons remains constant. However, this electron pair can be trapped by the repulsive potential of the antidot, so that the electrons will spend a long time colliding with this antidot. An example of the electron dynamics in this case is shown in Fig. 4. It shows that an electron can escape from the antidot even in the situation with  $\epsilon < \epsilon_c$ , when, without the interaction, the electrons remain trapped near the

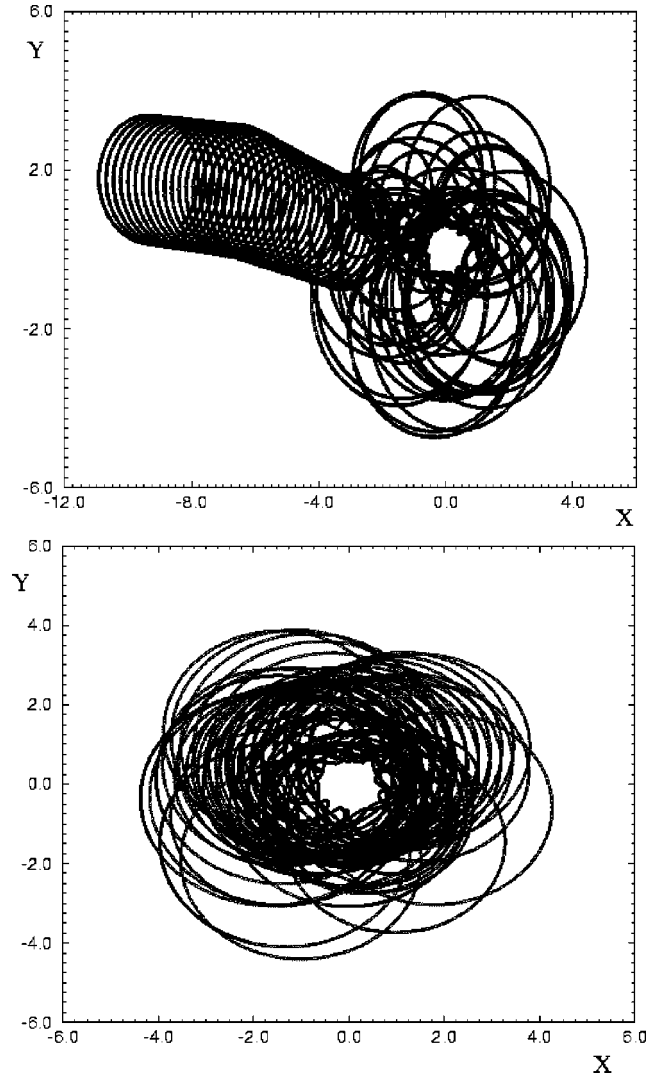


FIG. 4. Dynamics of two electrons in the  $(x, y)$  plane for  $H = 15.65$ ,  $B = -2.0$ ,  $E = 0.15$ , and  $\epsilon \approx 0.24$ , and an initial distance between electrons of  $|\mathbf{r}_1 - \mathbf{r}_2| \approx 0.5$ . After many cyclotron periods the first electron escapes from the antidot to infinity (upper figure), while the second remains trapped forever (bottom figure).

antidot. In our numerical simulations we observed different cases where one electron or both electrons escape to infinity.

To investigate how the escape rate depends on the strength of an external electric field  $E$ , we studied an ensemble of 100 paths. In each path the positions and momentums of each electron are chosen randomly in the intervals  $-4 \leq x, y \leq 4$ ,  $-2 \leq p_x, p_y \leq 2$  in such a way that the total energy is  $H \approx 15 \pm 0.5$ . We remind the reader that the antidot with potential (3) is placed at  $(0, 0)$  and  $U_0 = 1000$ . The escape rate  $\Gamma$  is defined as  $\Gamma = 1/T$ , where  $T$  is the time after which the distance of one of the electrons from the antidot is greater than  $R_{esc} \approx 5R_c \approx 10$ . This distance is sufficiently large, and as soon as it is reached an electron escapes to infinity and never returns to the antidot. The average value of  $\Gamma$  is obtained by averaging over 100 values obtained for 100 randomly chosen paths.

The dependence of the escape rate  $\Gamma$  on the strength of the applied electric field  $E$  is presented in Fig. 5. It definitely

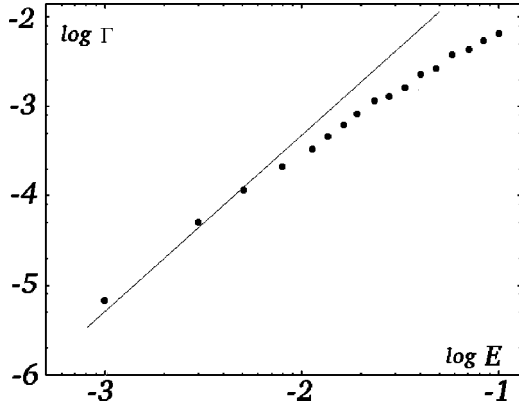


FIG. 5. Dependence of the escape rate  $\Gamma$  on the electric field  $E$  for electrons initially in the vicinity of the antidot at  $B = -2.0$ ,  $H \approx 15.0 \pm 0.5$ , and  $U_0 = 1000$ . Here, averaging is done over 100 paths,  $\omega_c = 2, \epsilon = 2\pi E/B^2$ , points give the numerical results for  $\Gamma$ , and the straight line gives the dependence [Eq. (6)]. Logarithms are decimal.

shows that the escape takes place even at very weak electric fields with  $\epsilon \ll \epsilon_c$ , when, without Coulomb interaction, electrons are forever trapped near the antidot. According to the obtained numerical data (see Fig. 5), in the limit of  $\epsilon \rightarrow 0$  the escape rate is

$$\Gamma/\omega_c \approx \epsilon^2. \quad (6)$$

Our understanding of this dependence is based on the following argument. Due to the Coulomb interaction between electrons, their dynamics in the vicinity of the antidot becomes chaotic. Therefore, the phase  $\phi$  in the map [Eqs. (4)] changes randomly between electron collisions with the antidot, and  $\beta$  grows diffusively with the number of collisions  $n$ , so that  $(\Delta\beta)^2 \approx Dn$ , with  $D = \epsilon^2/2$ . This diffusion results in the escape rate  $\Gamma/\omega_c \sim D \sim \epsilon^2$ , in agreement with the numerical data in Fig. 5.

#### IV. TWO-ELECTRON PROPAGATION IN ANTIDOT SUPERLATTICE

We also studied the electron dynamics on a square antidot superlattice, when the antidot potential is given by Eq. (3) and the distance between antidots is  $d > 2$ . In this case our results for one-electron dynamics are in qualitative agreement with the conclusions drawn in Refs. 5 and 6. As soon as the cyclotron radius  $R_c$  becomes comparable to the antidot spacing  $d$ , the trajectories start to move diffusively on the whole lattice. Trapped orbits near one antidot exist only for  $2R_c < d$  and  $\epsilon < \epsilon_c$ . For  $R_c > d/2$ , the cyclotron circle starts to drift in a way similar to that shown in Fig. 3. After a time  $t_d \sim d/v_d$ , a collision with another antidot takes place that finally originates a sequence of irregular jumps between antidots. The diffusion rate on the superlattice originated by this process can be estimated as  $D_{lat} \sim d^2/t_d \sim d v_d$ . This diffusion is important in the limit  $R_c \sim d \gg 1$ . However, we note that even at  $E = 0$ , at  $R_c > d/2$ , there are chaotic orbits which diffuse over the whole lattice, as discussed in detail in Refs. 5 and 6, and this diffusion is dominant for  $d \sim 1$ .

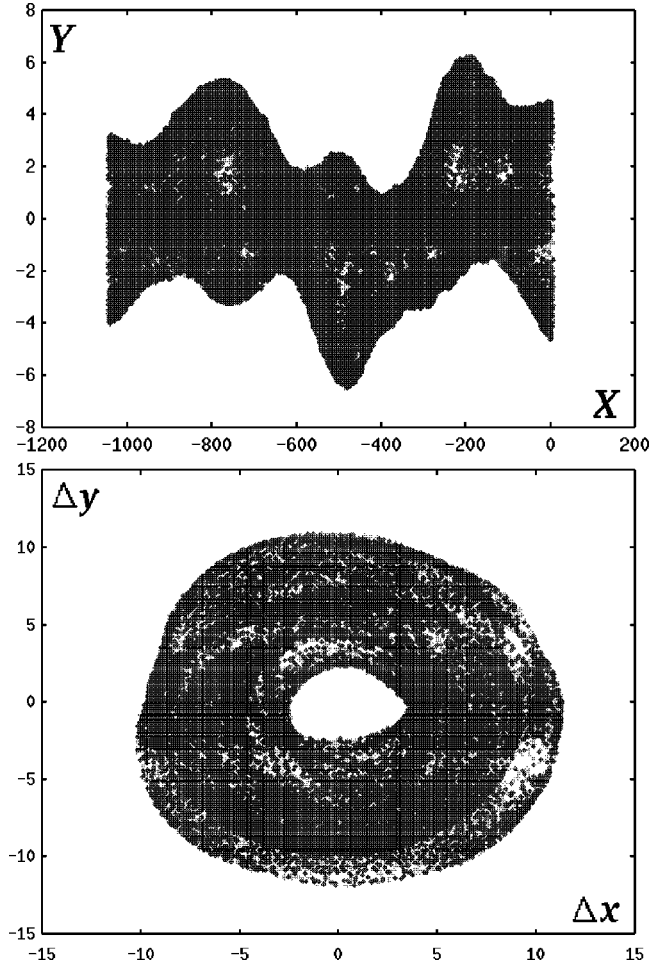


FIG. 6. Dynamics of two electrons in the  $(x, y)$  plane of an antidot superlattice for  $H \approx 51$ ,  $B = -2.0$ ,  $E = 0.4$ , and  $\epsilon \approx 0.63$  and initial distance between electrons  $|\mathbf{r}_1 - \mathbf{r}_2| \approx 4$ . The antidots are placed on a square superlattice with period 4 and  $U_0 = 1$  in Eq. (3). The upper figure shows the propagation of the first electron in the plane  $(x, y)$ , while the bottom figure shows the distance between the electrons  $\Delta x = x_1 - x_2$  and  $\Delta y = y_1 - y_2$ .

It is interesting to understand how two electrons move in such a superlattice. Intuitively, one would expect that the Coulomb repulsion would separate the electrons and that they would not propagate together. In fact, we found that this is not necessarily the case, and there are regimes where two electrons propagate together. An example of such a case is shown in Fig. 6. In this case the electron pair moves with an average drift velocity  $v_d \approx E/B$ , and the total displacement of the pair is about 100 times larger than the distance between the two electrons (Fig. 6).

The physical reason for the appearance of such electron pairs is quite clear in the absence of a superlattice potential. In this case, as discussed above at the beginning of Sec. III, electrons rotate around one another, and propagate together; their dynamics are integrable. Then, according to the KAM theorem, a weak perturbation will not destroy such pairs. Indeed, in the case of Fig. 6 the antidot potential is relatively weak ( $U_0 = 1 \ll H/2 \approx 25$ ), and the pair is not destroyed. We checked numerically that, provided  $U_0 \sim H/2$ , the pair size



starts to grow diffusively due to random scattering on a strong antidot potential, and eventually the pair is destroyed and electrons continue to propagate separately. For  $U_0 \gg H$ , the separation occurs after a few collisions with antidots. Conversely, for  $U_0 \ll H$ , the lifetime of the classical pair becomes infinite, in agreement with the KAM theorem.

## V. CONCLUSIONS

In this paper we investigated the effects of Coulomb interaction between two electrons on their classical dynamics in an antidot superlattice in crossed electric and magnetic fields. We found that for a weak electric field the electron pair can be trapped for a long time near an antidot, even if eventually one or two electrons escape from the antidot. The escape rate  $\Gamma$  decreases proportionally to the square of the electric field. This behavior is qualitatively different from the case of noninteracting electrons, which are trapped forever near the antidot in the limit of a small electric field.

The study of the electron pair dynamics in the antidot superlattice showed that the Coulomb repulsion can create stable pairs propagating for a large distance. In agreement with the KAM theorem, such pairs are stable when the antidot potential strength is relatively weak compared to the electron energy. Conversely, in the opposite limit the pairs become unstable, and electrons are quickly separated from one another. On the basis of this phenomenon it is possible to make a conjecture that in two-dimensional heterostructures with high mobility the impurity potential is relatively weak, and such electron KAM pairs will be stable and can be detected experimentally. We note that in recent experiments<sup>8</sup> with 2D electron gas, carriers of charge  $2e$  were detected. It is possible that these carriers are related to the KAM pairs found in this paper.

## ACKNOWLEDGMENT

We thank G. Casati, who pointed out the results found in Ref. 7.

---

<sup>1</sup>K. Ensslin and P. M. Petroff, Phys. Rev. B **41**, 12 307 (1990).

<sup>2</sup>D. Weiss, M. L. Roukes, A. Menschig, P. Grambow, K. von Klitzing, and G. Weimann, Phys. Rev. Lett. **66**, 2790 (1991).

<sup>3</sup>G. M. Gusev, V. T. Dolgoplov, Z. D. Kvon, A. A. Shashkin, V. M. Kudryashov, L. V. Litvin, and Yu. Nastaushchev, Pis'ma Zh. Eksp. Teor. Fiz. **54**, 369 (1991) [JETP Lett. **54**, 364 (1991)].

<sup>4</sup>M. V. Budantsev, Z. D. Kvon, A. G. Pogosov, G. M. Gusev, J. C. Portal, D. K. Maude, N. T. Moshegov, and A. I. Toropov, Physica B **256-258**, 595 (1998).

<sup>5</sup>R. Fleischmann, T. Geisel, and R. Ketzmerick, Phys. Rev. Lett. **68**, 1367 (1992).

<sup>6</sup>T. Geisel, R. Ketzmerick, and O. Schedletsky, Phys. Rev. Lett. **69**, 1680 (1992).

<sup>7</sup>N. Berglund, A. Hansen, E. H. Hauge, and J. Piasecki, Phys. Rev. Lett. **77**, 2149 (1996).

<sup>8</sup>D. C. Glattli, V. Rodriguez, H. Perrin, P. Roche, Y. Jin, and B. Etienne, Physica E **6**, 22 (2000).